Carbohydrate Polymers 77 (2009) 358–364

Contents lists available at ScienceDirect

Carbohydrate Polymers

journal homepage: www.elsevier.com/locate/carbpol

Structure and properties of starch/α-zirconium phosphate nanocomposite films

Haixia Wu [b], Changhua Liu [b], Jianguang Chen [b], Peter R. Chang [a,*], Yun Chen [a,c], Debbie P. Anderson [a]

[a] Bioproducts and Bioprocesses National Science Program, Agriculture and Agri-Food Canada, 107 Science Place, Saskatoon, SK, Canada S7N 0X2
[b] College of Chemistry and Chemical Engineering, Southwest University, 400715 Chongqing, China
[c] Department of Biomedical Engineering, School of Basic Medical Science, Wuhan University, Wuhan 430071, China

ARTICLE INFO

Article history:
Received 13 December 2008
Received in revised form 28 December 2008
Accepted 7 January 2009
Available online 14 January 2009

Keywords:
Thermoplastic starch
α-Zirconium phosphate
Nanocomposite films

ABSTRACT

Glycerol-plasticized pea starch/α-zirconium phosphate (PS/ZrP) nanocomposite films with different loading levels of α-zirconium phosphate (α-ZrP) were prepared by a casting and solvent evaporation method. The effects of the α-ZrP on the structure and properties of the PS/ZrP films were characterized by Fourier transform infrared (FT-IR) spectroscopy, wide-angle X-ray diffraction (XRD), scanning electron microscopy (SEM), thermogravimetric analysis (TGA) and tensile testing. The results indicated that hydrogen bonds formed between pea starch (PS) and α-ZrP, which improved the compatibility between PS and α-ZrP. Compared with the neat PS, the tensile strength (σ_b) and elongation at break (ε_b) of the PS/ZrP nanocomposite films were significantly enhanced with an increase in α-ZrP content. The maximum values of σ_b and ε_b reached 9.44 MPa and 47.5%, respectively, at 0.3% α-ZrP and 25% glycerol as plasticizer. The moisture uptake of the nanocomposite films, measured in an environment with 92% relative humidity, was reduced by the addition of α-ZrP. The structure and properties of pea starch-based films were modified and improved by the incorporation of α-ZrP.

Crown Copyright © 2009 Published by Elsevier Ltd. All rights reserved.

1. Introduction

Currently, environmentally friendly materials from natural and renewable resources have attracted enormous attention world wide from academics, industry, government and consumers as a result of concerns over environmental threats and the cost and supply of petroleum (Ishiaku, Pang, Lee, & Ishak, 2002; Jansson, Järnström, Rättö, & Thuvander, 2006; Ma & Yu, 2004; Nakamura, Cordi, Almeida, Duran, & Mei, 2005; Pracella, Pazzagli, & Galeski, 2002; Yu, Dean, & Li, 2006). Starch, an easily available, cheap and completely biodegradable polymer, has been considered one of the most promising raw materials and has been used in various fields such as agriculture, medicine and packaging (Funke, Bergthaller, & Lindhauer, 1998; Hulleman, Janssen, & Feil, 1998; Lu, Tighzerta, Dole, & Erre, 2005). Starch is a natural semicrystalline polymer composed of amylose and amylopectin. The amylose is almost linear, in which the repeating units are linked by α (1-4) linkages; the amylopectin has an α (1-4) linked backbone and about 5% α (1-6) linked branches (Cheetham & Tao, 1998; Svensson & Eliasson 1995). Starch therefore has three free hydroxyl groups in each glycoside ring.

Starch-based materials present two main disadvantages: poor mechanical properties and poor water resistance due to their hydrophilic nature, as compared with synthetic polymers, which limit their applications (Zhang et al., 2007). In order to improve the mechanical properties and water resistance, starch has been modified (Fringant, Desbrieres, & Rinaudo, 1996; Fringant, Rinaudo, Foray, & Bardet, 1998; Morikawa & Nishinari, 2000) or cross-linked (Chatakanonda, Varavinit, & Chinachoti, 2000; Dumoulin, Alex, Szabo, Cartilier, & Mateescu, 1998) using different methods. In the meantime, other strategies have been developed which include blending with synthetic (Arvanitoyannis, Biliaderis, Ogawa, & Kawasaki, 1998; Avérous & Fringant, 2001; Avérous, Moro, Dole, & Fringant, 2000; Psomiadou, Arvanitoyannis, Biliaderis, Ogawa, & Kawasaki, 1997; Sem & Bhattacharya, 2000; Sharma et al., 2001; Wu & Zhang, 2001) or natural polymers (Arvanitoyannis, Nakayama, & Aiba, 1998; Carvalho, Curvelo, & Agnelli, 2001; Fishman, Coffin, Konstance, & Onwulata, 2000; Xu, Kim, Hanna, & Nag, 2005).

Polymer/layered silicate nanocomposites exhibited improved physical and mechanical properties (Giannelis, 1996; Sanchez et al., 2001; Tsai et al., 2005; Wilhelm, Sierakowski, Souza, & Wypych, 2003). Clay minerals are the most widely used nanofiller for this purpose because of their special layered structure, high cation exchange capacity and low cost. However, the success of using clay minerals relies on the quality, specification and cost of high purity montmorillonite (MMT) refined from the naturally mined clay. In addition, the aspect ratio and particle size, which are very important for fine tuning the physical and mechanical properties of the composite, cannot be controlled in the MMT clay. On the other hand, synthetic α-zirconium phosphate (α-ZrP), i.e. $Zr(HPO_4)_2 \cdot H_2O$,

* Corresponding author. Tel.: +1 306 9567637; fax: +1 306 9567247.
E-mail address: Changp@agr.gc.ca (P.R. Chang).

0144-8617/$ - see front matter Crown Copyright © 2009 Published by Elsevier Ltd. All rights reserved.
doi:10.1016/j.carbpol.2009.01.002

which exhibits similar structural characteristics to natural MMT clay, is ideal for a fundamental structure–property relationship study of polymer nanocomposites. The advantages of α-ZrP as a model system over MMT clay include a much higher purity and ion exchange capacity and ease of intercalation and exfoliation (Clearfield & Berman, 1981; Clearfield, Duax, Garces, & Medina, 1972; Sun, Boo, Browning, Sue, & Clearfield, 2005). The particle size and aspect ratio can be manipulated by varying the reaction conditions. Such nanocomposites not only exhibit excellent mechanical and barrier properties, but also may possess proton conductivity when a proper matrix is selected (Costamagna, Yang, Bocarsly, & Srinivasan, 2002; Vaivars, Furlani, Mellander, & Granqvist, 2003; Yang, Srinivasan, Bocarsly, Tulyani, & Benziger, 2004). These proton conductive nanocomposites may find great applications in the fuel cell field. The application of α-ZrP as nanofiller in polymer matrices to prepare nanocomposites has been reported recently (Sue & Gam, 2004; Sue et al., 2004).

In this study, α-ZrP with a large interlayer spacing was synthesized to make PS/ZrP nanocomposites. For this purpose, α-ZrP was exfoliated using a commercially available *n*-butylamine. The resulting material was then incorporated into starch. The objective of this work was to study the effect of exfoliated α-ZrP nanoplatelets on the performance of thermoplastic starch films. The structure, thermal and mechanical properties of the α-ZrP nanocomposite films were studied by Fourier transform infrared (FT-IR) spectroscopy, wide-angle X-ray diffraction (XRD), scanning electron microscope (SEM), thermogravimetric analysis (TGA) and tensile testing. In addition, the relationship between the structure and properties of the nanocomposite films was also discussed.

2. Experimental method

2.1. Materials

Pea starch (PS), with an average granule size of 29 μm and composed of 35% amylose and 65% amylopectin, was obtained from Nutri-Pea Limited (Portage la Prairie, Manitoba, Canada). The plasticizer, glycerol (99%), was purchased from Maoye Chemical Company (Chongqing, China). Zirconium oxychloride octahydrate ($ZrOCl_2{\cdot}8H_2O$) (99%) was purchased from Tianjin Kermel Chemical Reagent Development Center (Tianjin, China). The prepared α-ZrP was exfoliated by *n*-butylamine (99%), which was supplied by Chengdu Kelong Chemical Reagent Company (Chengdu, China). Phosphoric acid was purchased from Chongqing Beibei Chemical Reagent Factory (Chongqing, China).

2.2. Synthesis and exfoliation of α-ZrP

The pristine α-ZrP was synthesized according to the procedure previously reported (Clearfield & Stynes, 1964) with a slight modification as follows: A gel was obtained by the addition of $ZrOCl_2{\cdot}8H_2O$ to 12 M phosphoric acid, followed by stirring and refluxing at 110 °C for 24 h.

The prepared α-ZrP was exfoliated very slowly by *n*-butylamine in an aqueous dispersion system (2 g/L) with a molar ratio of 2.5 (*n*-butylamine to α-ZrP). This was followed by a 1 h ultrasonic treatment and then stirred overnight at room temperature.

2.3. Film preparation

The glycerol-plasticized pea starch/α-zirconium phosphate nanocomposite films were fabricated by means of a casting and solvent evaporation process (Mathew, Brahmakumar, & Abraham, 2006). PS solutions (5 wt%) were prepared by dispersing native starch in distilled water with 25 wt% glycerol. The starch suspension was stirred at 95 °C for 30 min until the solution became transparent and a starch paste was obtained. The exfoliated α-ZrP was then added to the starch dispersion and stirring was continued for another 30 min at 60 °C. After degassing under vacuum, the composite was cast onto glass plates and then dried at 50 °C for 10 h to obtain dry films. By changing the exfoliated α-ZrP content to 0.1, 0.2, 0.3, 0.4 and 0.5 wt%, respectively, a series of nanocomposite films with a thickness of around 0.1 mm was prepared and coded as PS/ZrP-n (where n represents the exfoliated α-ZrP permillage content). For example, the film coded as PS/ZrP-1 showed that the permillage content of exfoliated α-ZrP based on dry starch content in the film was 1 wt‰ (i.e. 0.1 wt%). The codes of samples were listed in Table 1.

Table 1
Codes of the samples and temperature values of PS/ZrP-n nanocomposite films at maximum weight loss measured from TG.

Code	PS/ZrP-0	PS/ZrP-1	PS/ZrP-2	PS/ZrP-3	PS/ZrP-4	PS/ZrP-5
α-ZrP (%)	0	0.1	0.2	0.3	0.4	0.5
T_{max} (°C)	316.53	315.27	308.34	316.53	298.25	300.14

2.4. Fourier transform infrared (FT-IR) spectroscopy

Fourier transform infrared (FT-IR) spectroscopy of the nanocomposite was recorded with a Nicolet (Madison, WI, USA) 170SX Fourier transform infrared spectrometer in the wavelength range from 4000 to 400 cm^{-1}, in the attenuated total reflection mode.

2.5. X-Ray diffractometry (XRD)

X-ray diffraction (XRD) patterns of the samples were carried out with a XRD-3D, PuXi (Beijing, China) X-ray diffractometer under the following conditions: Nickel filtered CuKα radiation (λ = 0.15406 nm) at a voltage of 36 kV and current of 20 mA. The scanning rate was 4°/min in the angular range of 3–50° (2θ). The PS/ZrP-n nanocomposite films containing 25% glycerol were placed in desiccators and conditioned at 43% *RH* for 48 h before testing.

2.6. Scanning electron microscopy (SEM)

The PS/ZrP-n nanocomposite films containing 25% glycerol were fractured in liquid nitrogen and the cross-sections were mounted on SEM stubs with double sided adhesive tape, and then coated with gold in a 13.3 Pa vacuum degree. A scanning electron microscope (S-4800, HITACHI, Japan) was used to observe the morphologies of cross-sections of the films at an accelerating voltage of 0.5 kV. The morphology of the pristine α-ZrP powder was also observed at an accelerating voltage of 0.5 kV.

2.7. Thermogravimetric and differential thermogravimetry analysis

Thermogravimetric (TG) and differential thermogravimetric (DTG) analysis of the PS/ZrP-n nanocomposite films containing 25% glycerol was carried out on a TA-STDQ600 (TA Instruments Inc., New Castle, DE, USA). The thermograms were acquired between 20 and 500 °C at a heating rate of 10 °C/min. Nitrogen was used as the purge gas at a flow rate of 20 mL/min. An empty pan was used as a reference.

2.8. Transparency

Transparency of the PS/ZrP-n nanocomposite films containing 25% glycerol was obtained on an UV–vis spectrophotometer (UV-2550, Shimadzu (Suzhou) Instruments Manufacture Co., Ltd., Suzhou, China) in transmittance mode at wavelength from 250 to 800 nm.

2.9. Mechanical properties

The tensile strength and elongation at break of the films were determined using an universal testing machine (CMT 6500, Shenzhen Sans Testing Machine Co. Ltd., Shenzhen, China) according to the Chinese standard (GB 13022-91). The films were cut into 10 mm wide and 100 mm long strips and mounted between cardboard grips (150 × 300 mm) using adhesive so that the final area exposed was 10 × 50 mm. Before testing, the samples were kept at 43% *RH* for more than one week at room temperature to ensure equilibration of the moisture uptake in the films. The cross-head speed was 10 mm/min. All measurements were performed on three specimens and averaged.

2.10. Moisture uptake test

The moisture uptake of the PS/ZrP-n nanocomposite films containing 25% glycerol was determined. The samples used were thin rectangular strips with dimensions of 50 mm × 10 mm × 0.1 mm. They were dried overnight at 80 °C. After the samples were weighed, they were conditioned at 92% *RH* (Na_2CO_3 saturated solution) for two weeks to ensure equilibrium of the moisture before testing. The moisture uptake (*MU*) of the samples was calculated as follows:

$$MU = (W_1 - W_0)/W_0 \times 100\%$$

where W_0 and W_1 were the weight of the sample before exposure to 92% *RH* and after equilibrium, respectively. An average value of three replicates for each sample was taken.

3. Results and discussion

3.1. Fourier transform infrared spectroscopy

The FT-IR spectra of pristine α-ZrP and the films containing 25% glycerol are shown in Fig. 1. In the FT-IR spectra of pristine α-ZrP, the peaks at 3594, 3510, 3164 and 1620 cm^{-1} were attributed to the water symmetric and asymmetric stretching and bending vibrations. The peaks at 3384, 1251 and 597 cm^{-1} were assigned as P–OH stretching or deformation vibrations. The sharp band at 529 cm^{-1} was attributed to PO_2 deformation vibration. The strong bands in the range of 1000–1200 cm^{-1} are characteristic of PO_4 stretching vibrations (Zhang, Xu, Tang, & Gao, 1997). In pea starch film (PS/ZrP-0), the peak at 998 cm^{-1} was attributed to the characteristic absorption of C–O bond stretching. The band at 1642 cm^{-1} was assigned to the δ bending vibration of O–H. The sharp band at 2927 cm^{-1} is characteristic of C–H stretching associated with ring methane hydrogen atoms. An extremely broad band occurred at 3284 cm^{-1} due to hydrogen-bonded hydroxyl groups that contribute to the complex vibrations associated with free inter- and intramolecular bound hydroxyl groups, which make up the gross structure of starch (Mathew et al., 2006).

In the typical spectrum of the PS/ZrP-3 composite film, the characteristic peaks of pea starch at 998, 1642 and 3284 cm^{-1} have shifted to 996, 1650 and 3279 cm^{-1} respectively, indicating that there are hydrogen-bond interactions between the hydroxyl groups of PS and hydroxyl groups of α-ZrP, which have improved the compatibility between them.

3.2. X-Ray diffractometry

Fig. 2(a) shows the XRD patterns of the pristine α-ZrP (A) and the α-ZrP exfoliated by *n*-butylamine (B). The X-ray diffraction pattern of α-ZrP shows three characteristic peaks at $2\theta = 11.9°$, 20.1° and 25.4° in the angle range from 3° to 30°. The interlayer d-spacing of pristine α-ZrP is known to be 7.6 Å ($2\theta = 11.7°$) (Sue & Gam,

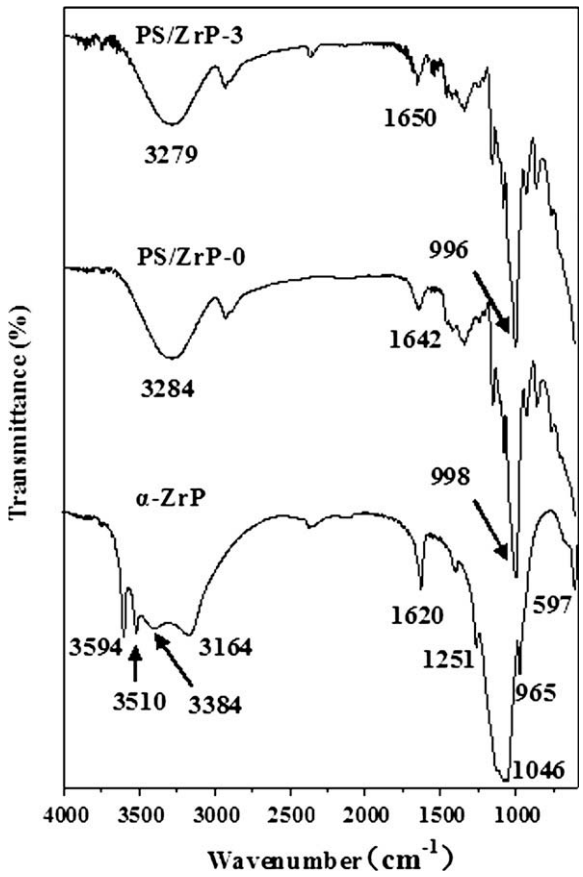

Fig. 1. FT-IR spectra of PS/ZrP-0, PS/ZrP-3 nanocomposite films and pristine α-ZrP powder.

2004). In this paper, the interlayer spacing of α-ZrP is about 7.4 Å ($2\theta = 11.9°$), which may be due to the high crystallinity of α-ZrP as a result of using high concentration phosphoric acid (12 M). When the α-ZrP has been exfoliated, the diffraction peak at 11.9° (7.4 Å) shifts to a lower Bragg's angle, 5.2° (16.8 Å), and a less intense peak at 9.9° (8.9 Å), which is in agreement with previous reports (Sun et al., 2005). The strong peak at 5.2° (16.8 Å) indicates that a large amount of α-ZrP nanoplatelets have been exfoliated and a less intense peak at 9.9° (8.9 Å) indicates that a small amount of α-ZrP crystals remained partially intercalated, which is similar to the previous report (Sun, Boo, Sun, Clearfield, & Sue, 2007).

As shown in Fig. 2(b), the XRD patterns of PS/ZrP-n nanocomposite films display a broad hump located around $2\theta = 18.0°$ with some low intensity diffraction peaks. For the PS/ZrP-0 film (neat starch film), the typical C-type crystallinity pattern with peaks at $2\theta = 5.7°$ (characteristic of B type polymorphs), 15.1° (characteristic of A type polymorphs), 17.2° (characteristic of both A and B type polymorphs), 20.18° and 22.58° (characteristic of B type polymorphs) can be observed clearly (Yoshimura, Takaya, & Nishinari, 1998). This shows that the addition of α-ZrP has no influence on the crystal type in the film, but the intensity of the diffraction peaks decreases. From PS/ZrP-0 to PS/ZrP-3, it can be clearly observed that the diffraction peaks at $2\theta = 5.7°$, 15.1°, 17.2°, 20.2° and 22.6° became broader with an increase in α-ZrP content. The intensity of the diffraction peak reached the minimum when the α-ZrP content was 0.3% (PS/ZrP-3), indicating the highest compatibility between starch and the α-ZrP. Because of the small size of α-ZrP, it easily disperses into the macromolecular chains and forms hydrogen bonds with starch, which restricts the movement of starch chains. When the α-ZrP content increased further (>0.3%), the diffraction peaks ($2\theta = 5.7°$, 15.1°, 17.2°, 20.2° and 22.6°) be-

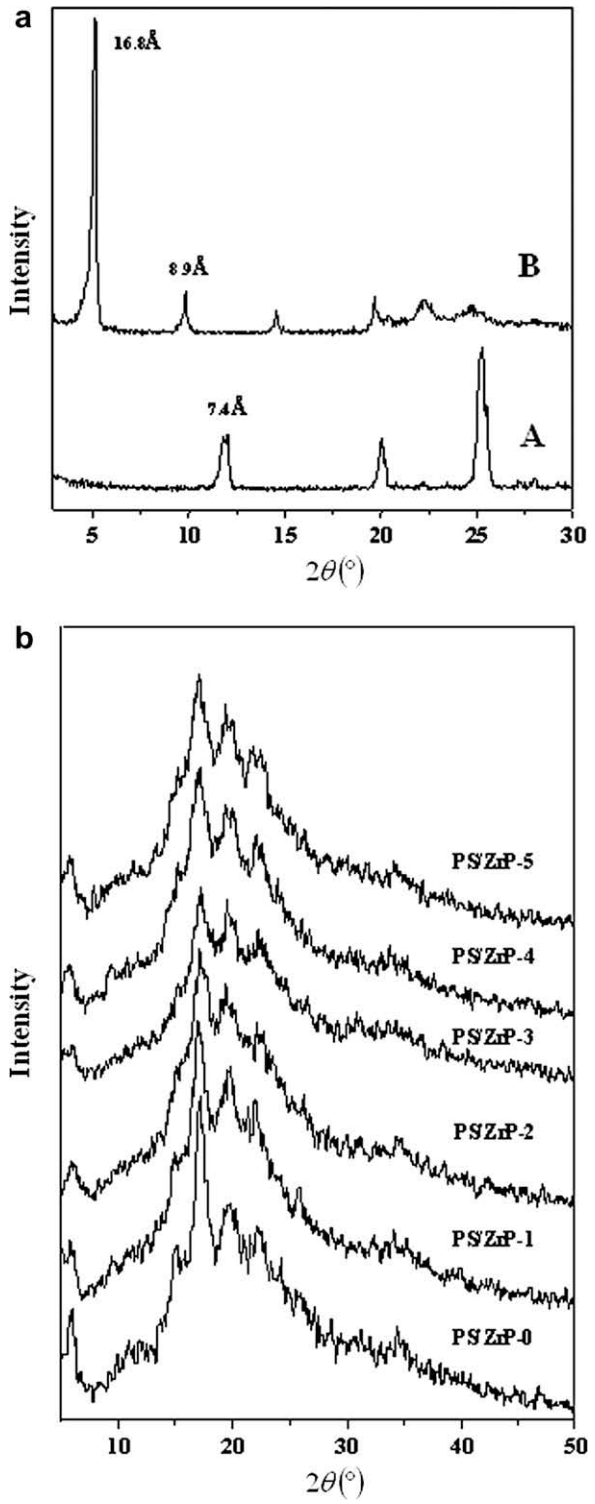

Fig. 2. (a) XRD patterns of the pristine α-ZrP powder (A) and α-ZrP powder exfoliated by *n*-butylamine (B). (b) XRD patterns of PS/ZrP-n nanocomposite films.

came sharp and the intensity gradually increased. The PS/ZrP-4 and PS/ZrP-5 samples exhibit relatively higher crystallinity than PS/α-ZrP-3. This can be attributed to a certain degree of phase separation between starch and α-ZrP in PS/ZrP-4 and PS/ZrP-5.

3.3. Scanning electron microscopy

Fig. 3 displays the SEM micrographs of α-ZrP powders and those of the fracture surfaces after tensile testing for the films. As shown in the SEM micrographs, the α-ZrP powder clearly shows a plate-like structure and regular cubic sheets indicating that its crystallinity is very high, which was also proven by XRD (Fig. 2(a)), while the neat starch film (PS/ZrP-0) has a smooth and compact surface. From the SEM micrographs of PS/ZrP-0 to PS/ZrP-3, with progressive increases in the α-ZrP content in the nanocomposite films, α-ZrP still dispersed uniformly in the starch matrix during the fabrication process. Several holes occurred on the fracture surface of the PS/ZrP-1 film which may have come from residual bubbles in the starch paste before casting. The fracture surfaces of the PS/ZrP-1, PS/ZrP-2 and PS/ZrP-3 films are compact, suggesting a good compatibility between α-ZrP and starch in these cases. Because the surface of the α-ZrP has plenty of hydroxyl groups, it is easy to form strong hydrogen bonds with starch macromolecules. However, the fracture surfaces of the PS/ZrP-4 and PS/ZrP-5 films became relatively rougher, indicating a certain degree of phase separation between starch and α-ZrP, resulting from poor dispersion and aggregation of α-ZrP nanoparticles as the α-ZrP content increased up to 0.4%. The SEM results correspond well with the XRD patterns.

3.4. Thermogravimetric and differential thermogravimetric analysis

The thermogravimetric (TG) and differential thermogravimetric (DTG) curves of the films, shown in Fig. 4(a) and (b), are used to determine the weight loss of the films as they are heated. The initial weight loss of all samples at approximately 100 °C is due to the evaporation of water, while the weight loss in the second range (250–350 °C) corresponds to a complex process including the dehydration of the saccharide rings and depolymerization (Mathew & Dufresne, 2002). The TG curves show that all samples are stable up to 275 °C, with a maximum rate of decomposition occurring at about 300 °C. The temperatures of maximum loss for all samples are listed in Table 1. As the α-ZrP content increases, the maximum thermal decomposition temperature of the nanocomposite films decreases, which can be observed in Fig. 4(b). This indicates that the thermo-stability of the PS-based films decreases with an increase in the amount of α-ZrP incorporated in the nanocomposite films. This could be attributed to the increase in acidity of α-ZrP with the increase in temperature, which induces the decomposition of the glycoside bonds.

3.5. Transparency

Film transparency is an effective index for providing information on the size of dispersed particles in the starch matrix. Particle sizes or aggregate domains larger than visible wavelength would obstruct light, leading to translucent or opaque films (Piyaporn, Duangdao, Duanghathai, & Kawee, 2007). Transparency may be affected by various factors, including film thickness, fortunately there was an insignificant difference in the average thickness of the film samples. Fig. 5 shows the percent transmittance values of film samples. From Fig. 5, the neat starch film presents the highest percent of transmittance, due to the absence of light blocking particles, followed by the PS/ZrP-3 film and PS/ZrP-1 film, respectively. This may be due to the aggregations of α-ZrP particles increasing slightly with an increase in α-ZrP content. In general, the larger the aggregation, the lower the light transmittance of the resultant films. The results of light transmittance measurement indicate that there is no obvious decrease in the transparency after the incorporation of α-ZrP into starch, especially when the α-ZrP content is equal to or less than 0.3%.

3.6. Mechanical properties

Mechanical properties resulting from the tensile test are shown in Fig. 6. It was observed that both the tensile strength (σ_b) and the elongation at break (ε_b) of the nanocomposite films are remarkably

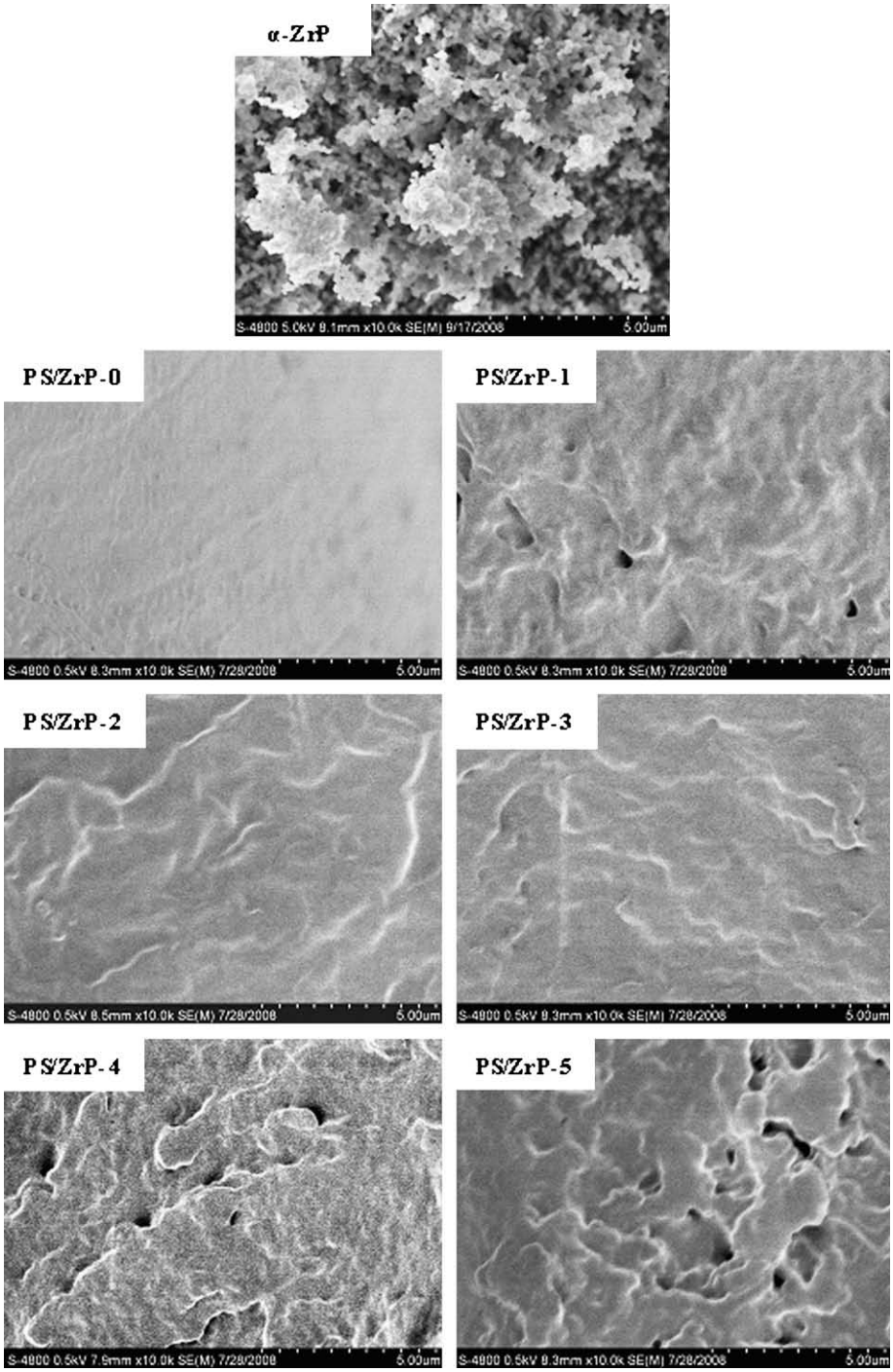

Fig. 3. SEM micrograph of the pristine α-ZrP powders and PS/ZrP-n nanocomposite films.

higher than those of the neat starch film (PS/ZrP-0). There is a stepwise increase in both σ_b and ε_b with the addition of α-ZrP. When 0.3% (PS/ZrP-3) of α-ZrP is added to the starch, the σ_b and the ε_b achieve the maximum values of 9.44 MPa and 47.5%, respectively. These results show that α-ZrP as filler in a polymeric matrix increases strength and flexibility of the starch, which is in agreement with findings from another study (Magaraphan, Lilayuthalert, Sirivat, & Schwank, 2001). The nanocomposites exhibit a remarkable improvement in mechanical properties. The main reason for the improvement in the mechanical properties is the stronger interfacial interaction between the matrix and α-ZrP due to the vast surface of the α-ZrP layers exposed.

3.7. Moisture uptake of the films

The moisture uptake (*MU*) of the nanocomposite films with different α-ZrP contents at 92% *RH* are plotted in Fig. 7. It was observed that the neat PS/ZrP-0 absorbs around 69.6 wt% moisture. Compared with the neat pea starch, the equilibrium moisture uptake was found to decrease with the addition of α-ZrP. This suggests that the addition of α-ZrP has an effect on the base polymers and formed hydrogen bonds between the molecules of starch and α-ZrP, decreasing the number of –OH groups available for interaction with migrating water molecules. This structure can reduce the diffusion of water mole-

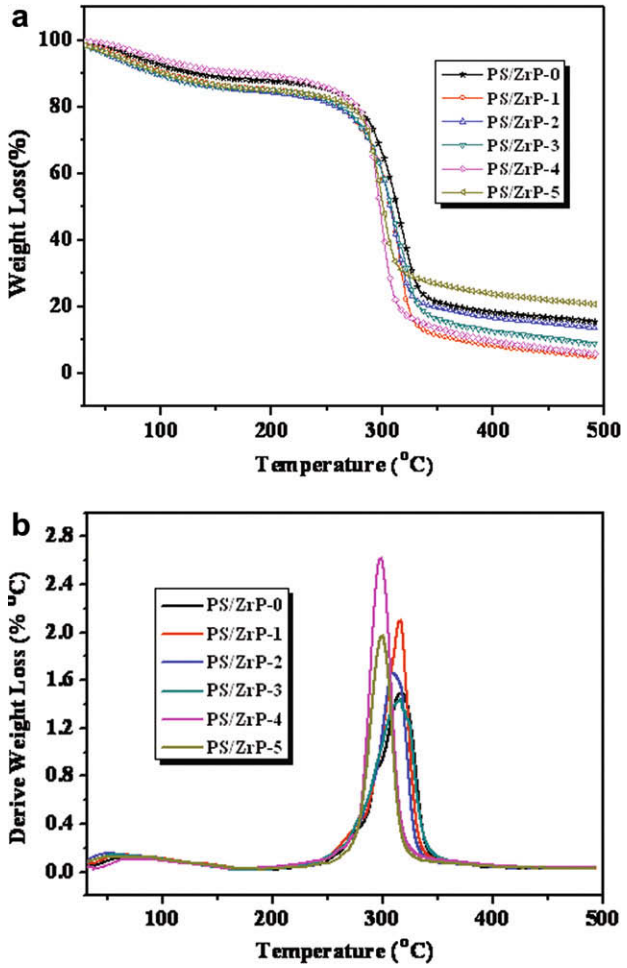

Fig. 4. (a) TG curves of PS/ZrP-n nanocomposite films. (b) DTG curves of PS/ZrP-n nanocomposite films.

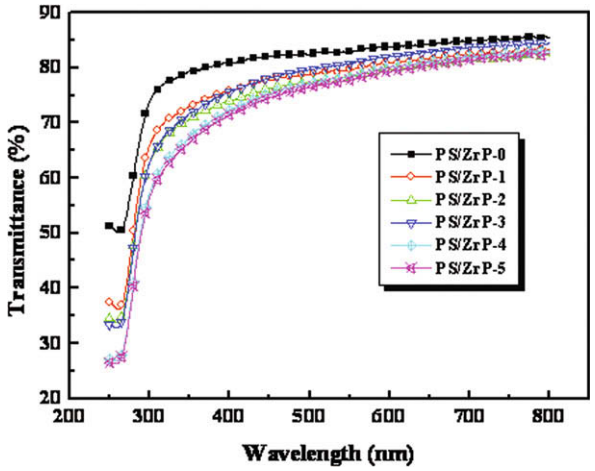

Fig. 5. Percent transmittance of PS/ZrP-n nanocomposite films.

cules in the material. The *MU* value reached the minimum value of 63.1 wt% when the α-ZrP content was 0.1 wt%. This may be due to the minimal number of –OH groups available for interaction with migrating water molecules. In addition, the *MU* at equilibrium increased as the α-ZrP content increased, when the α-ZrP content was higher than 0.1 wt%, and achieved saturation when the α-ZrP content was 0.5 wt%. This can be

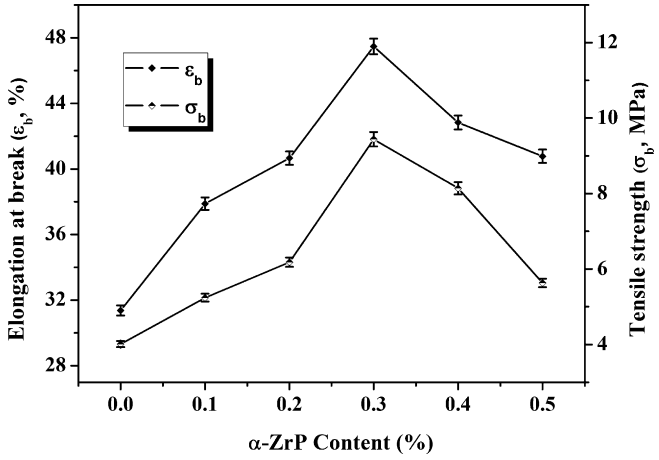

Fig. 6. Mechanical properties of PS/ZrP-n nanocomposite films with different α-ZrP content.

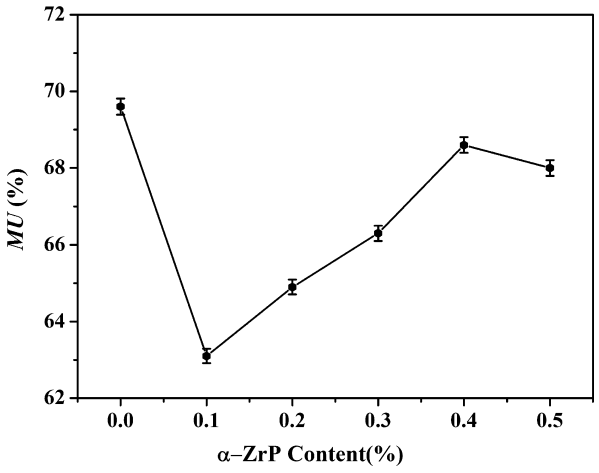

Fig. 7. Moisture uptake (*MU*) at equilibrium of the PS/ZrP-n nanocomposite films.

attributed to the increasing number of available –OH groups. However, all the values for moisture uptake of the nanocomposite films are lower than that of the neat PS film. These results indicate that the presence of α-ZrP improved the water resistance of pea starch.

4. Conclusions

A series of thermoplastic nanocomposite films was prepared from glycerol-plasticized pea starch (PS) and α-zirconium phosphate (α-ZrP). The results from XRD and SEM indicated that PS and α-ZrP interacted and formed strong hydrogen bonds, resulting in improved compatibility. With an increase in α-ZrP content, the maximum thermal decomposition temperature of the nanocomposite films decreased. The tensile strength of the films increased from 4.01 to 9.44 MPa as α-ZrP content increased from 0 to 0.3 wt% when 25 wt% glycerol was used as a plasticizer. It was worth noting that the values of elongation at break of the nanocomposite films were all higher than that of the neat PS film (PS/ZrP-0), and reached a maximum value of 47.5% when the α-ZrP content was 0.3 wt%. The presence of α-ZrP also decreased the moisture uptake of the nanocomposite films. The improvement to the properties of the PS/α-ZrP films may result from the hydrogen bonding formed between α-ZrP and PS molecules.

Acknowledgements

Authors are grateful to the CBIN program of Natural Resources Canada and Agricultural Bioproducts Innovation Program (ABIP) of Canada for partial funding of this project.

References

Arvanitoyannis, I., Biliaderis, C. G., Ogawa, H., & Kawasaki, N. (1998). Biodegradable films made from low-density polyethylene (LDPE), rice starch and potato starch for food packaging applications: Part 1. *Carbohydrate Polymers, 36*, 89–104.

Arvanitoyannis, I., Nakayama, A., & Aiba, S. I. (1998). Edible films made from hydroxypropyl starch and gelatin and plasticized by polyols and water. *Carbohydrate Polymers, 36*, 105–119.

Avérous, L., & Fringant, C. (2001). Association between plasticized starch and polyesters: Processing and performance of injected biodegradable systems. *Polymer Engineering and Science, 40*, 727–734.

Avérous, L., Moro, L., Dole, P., & Fringant, C. (2000). Properties of thermoplastic blends: Starch–polycaprolactone. *Polymer, 41*, 4157–4167.

Carvalho, A. J. F., Curvelo, A. A. S., & Agnelli, J. A. M. (2001). A first insight on composites of thermoplastic starch and kaolin. *Carbohydrate Polymers, 45*, 189–194.

Chatakanonda, P., Varavinit, S., & Chinachoti, P. (2000). Effect of crosslinking on thermal and microscopic transitions of rice starch. *Food Science and Technology, 33*, 276–284.

Cheetham, N. W. H., & Tao, L. (1998). Variation in crystalline type with amylase content in maize starch granules: An X-ray powder diffraction study. *Carbohydrate Polymer, 36*, 277–284.

Clearfield, A., & Berman, J. R. (1981). On the mechanism of ion exchange in zirconium phosphates–XXXIV. Determination of the surface areas of α-$Zr(HPO_4)_2{\cdot}H_2O$ by surface exchange. *Journal of Inorganic and Nuclear Chemistry, 43*, 2141–2142.

Clearfield, A., Duax, W. L., Garces, J. M., & Medina, A. S. (1972). On the mechanism of ion exchange in crystalline zirconium phosphates-IV potassium ion exchange of α-zirconium phosphate. *Journal of Inorganic and Nuclear Chemistry, 34*, 329–337.

Clearfield, A., & Stynes, J. A. (1964). The preparation of crystalline zirconium phosphate and some observations on its ion exchange behaviour. *Journal of Inorganic and Nuclear Chemistry, 26*, 117–129.

Costamagna, P., Yang, C., Bocarsly, A. B., & Srinivasan, S. (2002). Nafion® 115/zirconium phosphate composite membranes for operation of PEMFCs above 100 °C. *Electrochimica Acta, 47*, 1023–1033.

Dumoulin, Y., Alex, S., Szabo, P., Cartilier, L., & Mateescu, M. A. (1998). Cross-linking amylose as matrix for drug controlled release. X-ray and FTIR structural analysis. *Carbohydrate Polymers, 37*, 361–370.

Fishman, M. L., Coffin, D. R., Konstance, R. P., & Onwulata, C. I. (2000). Extrusion of pectin/starch blends plasticized with glycerol. *Carbohydrate Polymers, 41*, 317–325.

Fringant, C., Desbrieres, J., & Rinaudo, M. (1996). Physical properties of acetylated starch-based materials: Relation with their molecular characteristics. *Polymer, 37*, 2663–2673.

Fringant, C., Rinaudo, M., Foray, M. F., & Bardet, M. (1998). Preparation of mixed esters of starch or use of an external plasticizer: Two different ways to change the properties of starch acetate films. *Carbohydrate Polymers, 35*, 97–106.

Funke, U., Bergthaller, W., & Lindhauer, M. G. (1998). Processing and characterization of biodegradable products based on starch. *Polymer Degradation and Stability, 59*, 293–296.

Giannelis, E. P. (1996). Polymer layered silicate nanocomposites. *Advanced Materials, 8*, 29–35.

Hulleman, S. H. D., Janssen, F. H. P., & Feil, H. (1998). The role of water during plasticization of native starches. *Polymer, 39*, 2043–2048.

Ishiaku, U. S., Pang, K. W., Lee, W. S., & Ishak, Z. A. M. (2002). Mechanical properties and enzymic degradation of thermoplastic and granular sago starch filled poly(ε-caprolactone). *European Polymer Journal, 38*, 393–401.

Jansson, A., Järnström, L., Rättö, P., & Thuvander, F. (2006). Physical and swelling properties of spray-dried powders made from starch and poly(vinyl alcohol). *Starch/Stärke, 58*, 632–641.

Lu, Y., Tighzerta, L., Dole, P., & Erre, D. (2005). Preparation and properties of starch thermoplastics modified with waterborne polyurethane from renewable resources. *Polymer, 46*, 9863–9870.

Ma, X. F., & Yu, J. G. (2004). The plasticizers containing amide groups for thermoplastic starch. *Carbohydrate Polymers, 57*, 197–203.

Magaraphan, R., Lilayuthalert, W., Sirivat, A., & Schwank, J. W. (2001). Preparation, structure, properties and thermal behaviour of rigid-rod polyimide/montmorillonite nanocomposites. *Composites Science and Technology, 61*, 1253–1264.

Mathew, A. P., & Dufresne, A. (2002). Morphological investigation of nanocomposites from sorbitol plasticized starch and tunicin whiskers. *Biomacromolecules, 3*, 609–617.

Mathew, S., Brahmakumar, M., & Abraham, T. E. (2006). Microstructural imaging and characterization of the mechanical, chemical, thermal, and swelling properties of starch–chitosan blend films. *Biopolymers, 82*, 176–187.

Morikawa, K., & Nishinari, K. (2000). Rheological and DSC studies of gelatinization of chemically modified starch heated at various temperatures. *Carbohydrate Polymers, 43*, 241–247.

Nakamura, E. M., Cordi, L., Almeida, G. S. G., Duran, N., & Mei, L. H. I. (2005). Study and development of LDPE/starch partially biodegradable compounds. *Journal of Materials Processing Technology, 162–163*, 236–241.

Piyaporn, K., Duangdao, A., Duanghathai, P., & Kawee, S. (2007). Preparation of cassava starch/montmorillonite composite film. *Carbohydrate Polymers, 67*, 155–163.

Pracella, M., Pazzagli, F., & Galeski, A. (2002). Reactive compatibilization and properties of recycled poly(ethylene terephthalate)/polyethylene blends. *Polymer Bulletin, 48*, 67–74.

Psomiadou, E., Arvanitoyannis, I., Biliaderis, C. G., Ogawa, H., & Kawasaki, N. (1997). Biodegradable films made from low density polyethylene (LDPE), wheat starch and soluble starch for food packaging applications. Part 2. *Carbohydrate Polymers, 33*, 227–242.

Sanchez, C., Soler-Illia, G. J. A. A., Ribot, F., Lalot, T., Mayer, C. R., & Cabuil, V. (2001). Designed hybrid organic-inorganic nanocomposites from functional nanobuilding blocks. *Chemistry of Materials, 13*, 3061–3083.

Sem, A., & Bhattacharya, M. (2000). Residual stress and density gradient in injection molded starch/synthetic polymer blends. *Polymer, 41*, 9177–9190.

Sharma, N., Chang, L. P., Chu, Y. L., Ismail, H., Ishiaku, U. S., & Ishaki, Z. A. M. (2001). A study on the effect of pro-oxidant on the thermo-oxidative degradation behaviour of sago starch filled polyethylene. *Polymer Degradation and Stability, 71*, 381–393.

Sue, H.-J., & Gam, K. T. (2004). Epoxy nanocomposites based on the synthetic – zirconium phosphate layer structure. *Chemistry of Materials, 16*, 242–249.

Sue, H.-J., Gam, K. T., Bestaoui, N., Clearfield, A., Miyamoto, M., & Miyatake, N. (2004). Fracture behavior of α-Zirconium phosphate-based epoxy nanocomposites. *Acta Materialia, 52*, 2239–2250.

Sun, L., Boo, W. J., Browning, R. L., Sue, H.-J., & Clearfield, A. (2005). Effect of crystallinity on the intercalation of monoamine in α-zirconium phosphate layer structure. *Chemistry of Materials, 17*, 5606–5609.

Sun, L., Boo, W. J., Sun, D., Clearfield, A., & Sue, H.-J. (2007). Preparation of exfoliated epoxy/α-zirconium phosphate nanocomposites containing high aspect ratio nanoplatelets. *Chemistry of Materials, 19*, 1749–1754.

Svensson, E., & Eliasson, A. C. (1995). Crystalline changes in native wheat and potato starches at intermediate water levels during gelatinization. *Carbohydrate Polymer, 26*, 171–176.

Tsai, T. Y., Li, C. H., Chang, C. H., Cheng, W. H., Hwang, C. L., & Wu, R. J. (2005). Preparation of exfoliated polyester/clay nanocomposites. *Advanced Materials, 17*, 1769–1773.

Vaivars, G., Furlani, M., Mellander, B. E., & Granqvist, C. G. (2003). Proton-conducting zirconium phosphate/poly(vinyl acetate)/glycerine gel electrolytes. *Journal of Solid State Electrochemistry, 7*, 724–728.

Wilhelm, H.-M., Sierakowski, M. R., Souza, G. P., & Wypych, F. (2003). Starch films reinforced with mineral clay. *Carbohydrate Polymers, 52*, 101–110.

Wu, Q. X., & Zhang, L. N. (2001). Structure and properties of casting films blended with starch and waterborne polyurethane. *Journal of Applied Polymer Science, 79*(11), 2006–2013.

Xu, Y. X., Kim, K. M., Hanna, M. A., & Nag, D. (2005). Chitosan–starch composite film: preparation and characterization. *Industrial Crops and Products, 21*, 185–192.

Yang, C., Srinivasan, S., Bocarsly, A. B., Tulyani, S., & Benziger, J. B. (2004). A comparison of physical properties and fuel cell performance of Nafion and zirconium phosphate/Nafion composite membranes. *Journal of Membrane Science, 237*, 145–161.

Yoshimura, M., Takaya, T., & Nishinari, K. (1998). Rheological studies on mixtures of corn starch and konjac-glucomannan. *Carbohydrate Polymers, 35*, 71–79.

Yu, L., Dean, K., & Li, L. (2006). Polymer blends and composites from renewable resources. *Progress in Polymer Science, 31*, 576–602.

Zhang, H., Xu, J. S., Tang, Y., & Gao, Z. (1997). Studies on synthesis and properties of layered zirconium phosphate. *Chemical Journal of Chinese Universities, 18*, 172–176.

Zhang, S. D., Zhang, Y. R., Zhu, J., Wang, X. L., Yang, K. K., & Wang, Y. Z. (2007). Modified corn starches with improved comprehensive properties for preparing thermoplastics. *Starch/Stärke, 59*, 258–268.